EXPERIMENTAL INVESTIGATION AND MODELING OF THE ELECTRICAL RESPONSE OF THINLY LAYERED SHALY-SANDS (20 MHZ – 1 GHZ)

M. Pirrone[1], N. Bona[1], M.T. Galli[1], F. Pampuri[1],
N. Seleznev[2], M. Han[2], L. Mosse[2], O. Faivre[2], M. Hizem[2]
[1] Eni e&p, [2] Schlumberger

This paper was prepared for presentation at the International Symposium of the Society of Core Analysts held in Austin, Texas, USA 18-21 September, 2011

ABSTRACT
A physical model that relates high frequency conductivity and permittivity of shaly-sands to water content, water salinity and cation exchange capacity is verified against measurements conducted on more than 150 shaly-sand samples in the 20 MHz – 1 GHz frequency range. The aim of the study is to develop a frame for the interpretation of dielectric log data acquired in turbiditic shale-sand laminations with thicknesses down to a few centimeters. We describe the model, discuss the experiments and present two case studies.

INTRODUCTION
The exploration and production of thinly layered shaly-sand reservoirs, where bed thickness is well below the resolution capabilities of standard logging tools, require fit-for-purpose technology and interpretation methodologies. Turbiditic shale-sand sequences can be particularly critical, having thicknesses in the order of a few centimeters. In these systems, most logging tools merely provide estimations of average porosity and water saturation, and the risk of missing economic hydrocarbon-bearing layers becomes high. A new dielectric log that measures the electrical response (conductivity and dielectric permittivity) of rock at four different frequencies in the 20 MHz – 1 GHz range, with 1 inch vertical resolution, has been tested with the aim to obtain reliable information on pay, porosity, water saturation and clay content [**1**].
This paper discusses the extensive experimental and theoretical study performed in order to develop an interpretation model for this log. The following tasks were accomplished: (1) creation of a statistically representative database containing conductivity and permittivity spectra, mineralogical and petrophysical data from more than 150 core samples (Berea sandstones, artificially compacted clays, shaly-sand samples from various fields); (2) development of a physical model that relates the measured spectra to water content, water salinity and clay content; (3) verification of the theoretical model against the measurements and definition of its main limitations and validity range for use in log interpretation; (4) application of the model to real cases. The analytical model was adapted from that of Stroud, Milton and De [**2**] and has the advantage of being physically meaningful, taking into account geometrical and textural characteristics in the simplest

way and minimizing the number of unknowns. We believe that significant uncertainty reductions in the estimation of Hydrocarbons-In-Place in thinly layered reservoirs will be achieved thanks to this study.

Before describing the model and discussing the experiments, it may be useful to illustrate some basic concepts of dielectric dispersion. Rock electromagnetic properties usually refer to electrical conductivity (σ) and dielectric constant, or relative permittivity (ε). Mathematically, ε and σ are treated as part of a complex quantity called "complex permittivity". This is defined as $\varepsilon^* = \varepsilon + \iota\,\sigma/(\omega\varepsilon_0)$, where $\omega = 2\pi f$ is the angular frequency of the electric field, ε_0= 8.854 pF/m is the vacuum permittivity and $\iota = \sqrt{-1}$ is the imaginary unit. Throughout the paper, we use the superscript * to denote a complex quantity. The real part of ε^* is a measure of how much energy from the electric field is stored in the material; the imaginary part measures how dissipative or lossy the material is in relation to the electric field. **Fig.1** shows the trends of the two quantities as a function of frequency of a hypothetical external electric field when a polarization mechanism is active. This frequency dependence is normally called "dielectric dispersion".

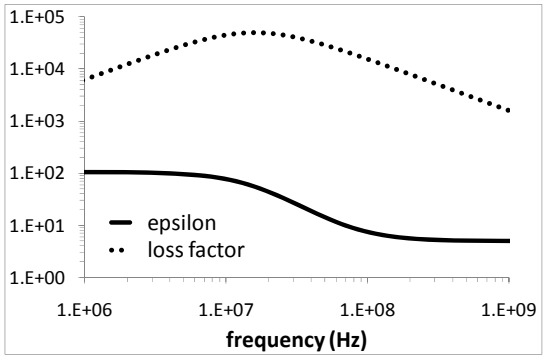

Figure 1: Frequency response of a generic polarization mechanism. At low frequencies the alternating electric field is slow enough so that the charges are able to follow the field variations. Because the polarization is able to develop fully, ε assumes its highest value and the loss factor $\sigma/(\omega\varepsilon_0)$ is low. As frequency increases, losses start to increase and ε begins to decrease due to the phase lag between the fluctuations of the charges and the electric field. A peak in the losses is observed at the so-called resonance frequency. At higher frequencies, ε and the loss factor are no longer dependent on frequency because the electric field is too fast to influence the movement of the charges and the polarization disappears.

THE MODEL

The generalized structure of a shaly-sand is sketched in **Fig.2**. Basically, it can be divided into two subgroups: solid particles (sand and clay) and pores (variably filled by brine and/or hydrocarbon). The clay mineral fraction can exist as either discrete particles or coatings on coarser particles. Fluids can be classified as: (1) hydrocarbon (oil and/or gas); (2) free and capillary water; (3) clay bound water. No distinction is made between free (i.e. movable) water and capillary water (water retained in small pores by capillarity) because they are electrically indistinguishable.

Our goal is to describe the dielectric response of this composite system using a suitable mixing model, i.e. a relation, ideally of an analytic form, which connects the complex dielectric permittivity of the composite to the complex permittivities and the relative volume fractions of its individual components. In fact, almost all existing mixing models use groups of components (or phases) rather than the individual components. We have tested different ways of clustering the individual components and have eventually come up to a 2-phase model consisting of a conducting phase (components 2 + 3 in **Fig.2**) and an insulating phase (components 1 + 4 + 5 in **Fig.2**).

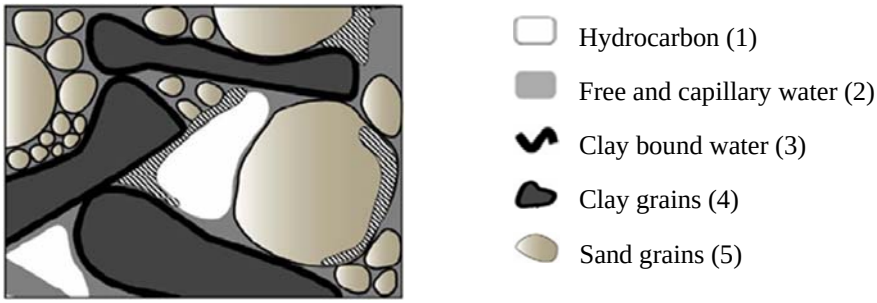

Figure 2: Schematic representation of a shaly sanstone and its 5 components (adapted from [**3**]).

The interactions between these two phases are mimicked using the model of Stroud-Milton-De (SMD) [**2**], a mathematically elegant theory that states that the effective complex permittivity of a 2-phase heterogeneous material can be written as a function of the ratio of the permittivity of one of the phases to that of the other, and in terms of a geometrical function, called spectral density function, which is determined by the shape and distribution of the interfaces present in the material. Unlike the majority of existing models [**4-6**], which introduce non-measurable microscopic parameters that undermine the robustness of the inversion process, the SMD model fulfils the following five requirements, which we deem indispensable: (1) it is reasonably simple to manage; (2) physically meaningful; (3) takes into account the geometry of the two phases in the simplest way; (4) minimizes the number of unknowns; (5) is able to reproduce the measured spectra.

Our formulation of the SMD model considers an insulating matrix (dry rock + hydrocarbon) with a purely real permittivity ε_r hosting an effective brine (free + capillary + clay bound water) with complex permittivity ε_w^*. The average complex permittivity ε^* of the whole system is expressed as a function of these two quantities plus another two, namely the water filled porosity ϕ_w and a textural/lithological parameter called μ. Mathematically, ε^* is given by:

$$1 - \frac{\varepsilon^*}{\varepsilon_r} = \frac{A_w}{s^*} + \int_0^1 \frac{g_w(n)}{s^* - n} dn$$

where $s^* = (1 - \varepsilon_w^*/\varepsilon_r)^{-1}$, $A_w = (\phi_w)^\mu$ and $g_w(n) = C(n)^{-b}(1-n)^e$ is the spectral density function representing the intensity, both in number and strength, of the various resonances related to the water phase ($n \in (0,1)$ is called the depolarization factor and C, e, b are functions of ϕ_w and A_w, namely: $C = (\phi_w - A_w)\frac{\Gamma(2-b+e)}{\Gamma(1-b)\Gamma(1+e)}$, $e = \frac{\phi_w(\phi_w - A_w)}{2\phi_w - A_w(3-\phi_w)}$ and $b = 1 - \frac{\phi_w(1-\phi_w)}{2\phi_w - A_w(3-\phi_w)}$, where $\Gamma(x) = \int_0^\infty t^{x-1}exp(-t)dt$ is the Euler's Gamma function).

In the end, dielectric dispersion measurements are reconciled with the model to extract the water volume fraction ϕ_w, the water salinity X_w (related to water conductivity) and μ. Despite its apparently high complexity, the model is actually quite simple in that it does not contain purely adjustable parameters: ϕ_w and X_w have a clear physical meaning

and, therefore, inversion results are easily controllable; μ is a sort of generalized Archie exponent which tends to Archie-*m* for clay free, fully water saturated rocks (the quantity $(\phi_w)^\mu$ is the low-frequency limit of the ratio between the overall rock conductivity and the effective water conductivity). The inversion scheme is (**Fig.3**):

$$(\varepsilon_{meas}, \sigma_{meas})_f = F(\varepsilon_r, \phi_w, \varepsilon_w^*, \mu)$$

with $\varepsilon_w^* = G(X_w, P, T, f)$. Here ε_{meas} and σ_{meas} are the measured permittivity and conductivity, F is the model, f represents the measurement frequency (four frequencies are available for the tool we are considering), G is an equation that relates the complex permittivity of water to the water salinity X_w, the pressure P and the temperature T. Pressure and temperature are measured independently. The effective matrix permittivity ε_r is fixed in the inversion process and comes from mineralogical considerations and theoretical permittivities.

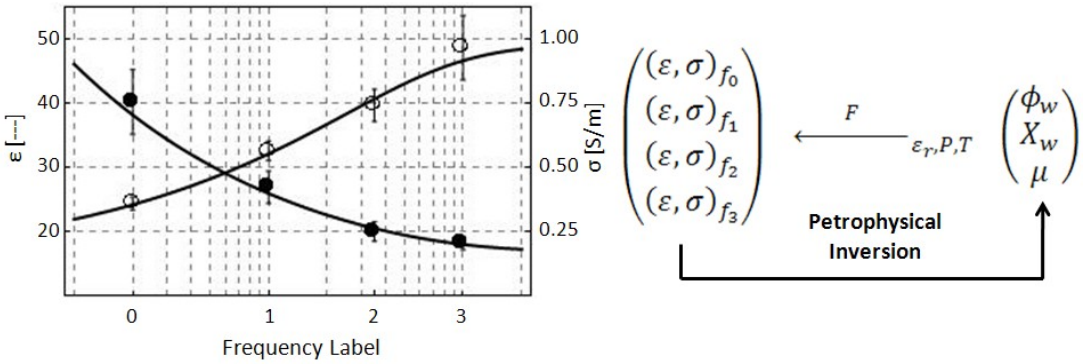

(a) **(b)**

Figure 3: Petrophysical inversion example and scheme. The filled circles are the measured permittivities while the open ones are the measured conductivities, all with the associated uncertainties. The four permittivities and four conductivities are fitted all together with the petrophysical model: the black curves represent the model's best fit to the measurements given their individual uncertainties (**Fig.3a**). The final output is the set of water-filled porosity, water salinity and μ parameter (**Fig.3b**). f_0, f_1, f_2 and f_3 are the four measuring frequencies.

It is worth mentioning that big efforts were done in order to explore the sensitivity of the model and to properly select the set of parameters to invert for. In particular, we investigated the possibility of inverting also for total porosity (or water saturation) in addition to ϕ_w. The main conclusions of the analysis are: (1) inverting for more than three parameters is not robust; (2) each time total porosity and ε_r are inverted together, the uncertainty on the output becomes large, as these two parameters are degenerated together.

EXPERIMENTAL STUDY

We performed experiments on three types of rocks:

1. Reservoir samples. These represent the majority of our database. The samples were taken from the Northern Italy onshore, Sicily offshore and Adriatic Sea basin. The investigated reservoirs are all gas-bearing sands and have formation water salinities

above 30 ppk. Clay percentages vary from zero to 50%. The shales were preserved and measured under fully saturated conditions, while sands and shaly-sands were cleaned, saturated with synthetic formation brine, and measured both under fully and partially saturated conditions.

2. Berea sandstone samples. Measurements were carried out on fully and partially saturated plugs taken from 150 md and 700 md cores.
3. Pure clay samples. These were created artificially by compacting dry clay grains under brine and filtering out the brine in excess. Four types of clays were used: a low Cation Exchange Capacity (CEC) kaolinite, a low CEC yellow illite, a medium CEC green illite, and a high CEC montmorillonite. Globally CEC values ranged from 4 to 90 meq/100g. In order to investigate the effects of water salinity on dielectric dispersion, different saturant water salinities were used: 1, 10 and 30 ppk.

Porosity and grain density/size, CEC, mineralogical content (from either X-Ray diffraction or IR spectroscopy), electrical conductivity and dielectric permittivity were measured on the available samples. **Fig.4** illustrates how porosity, CEC and the mica/clay fraction are distributed throughout the database. Conventional procedures were used for these determinations, so we do not go into details. The conductivity and permittivity spectra were obtained as a function of frequency in the 10 MHz – 20 GHz range from reflectometry measurements in an open-ended configuration (**Fig.5**). Eight measurements were performed on each sample. Their repeatability was found to be within 5% for 2/3 of the samples and within 10% for 95% of the samples.

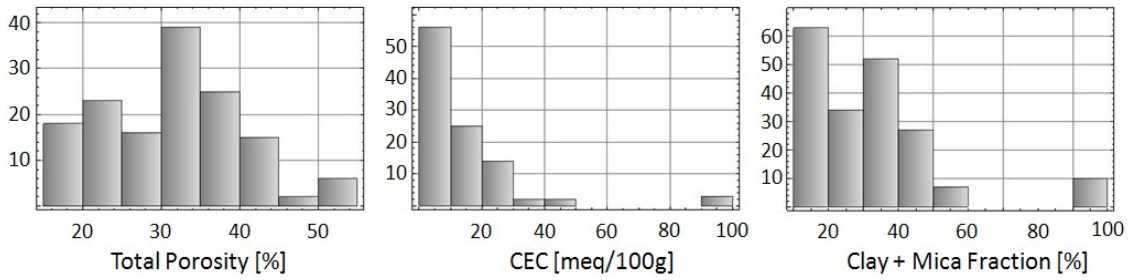

Figure 4: Total porosity, CEC and XRD-derived Clay + Mica fraction.

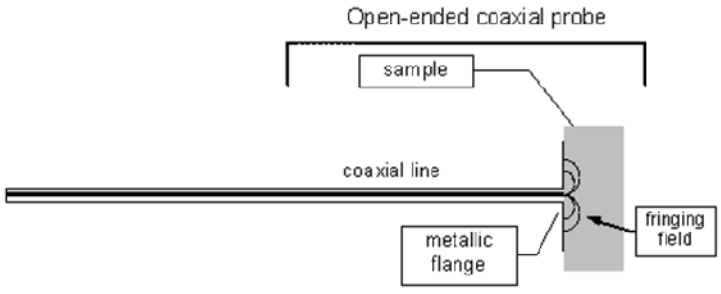

Figure 5: Schematic of the dielectric measurement. The open-ended coaxial probe is connected to the sample under test on one side and to an impedance analyzer (not shown here) on the other side. The complex permittivity of the sample is obtained from a measurement of the complex reflection coefficient. Calibrations were made by suspending the probe in air, immersing it under distilled water, and short-circuiting the line. The measurements were performed using two impedance analyzers (Agilent HP8722D and Agilent 4991A) and the Agilent 85070E coaxial probe.

VALIDATION OF THE MODEL AGAINST DATA

In their original paper, Stroud, Milton and De [**2**] proposed an analytical mixing formula for the limiting case of a clay free, fully water saturated rock (a two-component composite). The model was shown to be in agreement with experimental data over a broad range of frequencies for a variety of rock types. We confirm this nice behavior also in Berea sandstone: the fitting results are almost perfect (**Fig.6**) and the inverted values of water filled porosity and water salinity are very close to the true values (**Tab.1**). As can be seen, also partially water saturated samples can be modeled with success, and when Sw=100% the μ parameter is close to the Archie *m* exponent as expected.

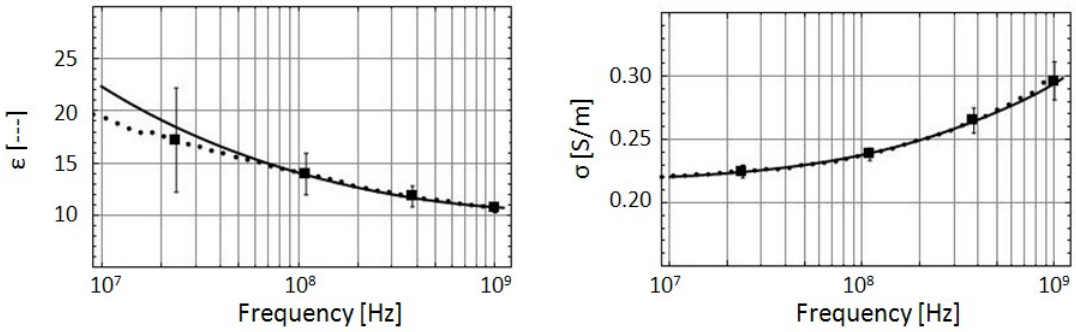

Figure 6: SMD best fit for a 700 md Berea sample: permittivity on the left and conductivity on the right. The dotted curves represent the measured data, while the continuous curves are the model's best fit to the measurements. The squares correspond to the permittivities and conductivities at the four tool frequencies (input for the inversion process).

	Water-filled porosity (%)		**Water salinity (ppk)**		**μ**	***m***
	Experimental	**SMD**	**Experimental**	**SMD**	**SMD**	**Archie**
Berea 150 md – Sw=100%	19	18	32	32	1.75	1.71
Berea 700 md – Sw=100%	23	22	32	30	1.68	1.62
Berea 150 md – Sw=51%	10	11	32	35	1.77	1.71
Berea 150 md – Sw=58%	11	12	32	39	1.81	1.71

Table 1: SMD inversion results for Berea samples having permeabilities of 150 and 700 md. The *m* exponent in the last column is given by standard low frequency resistivity measurements.

At the other end of the spectrum, pure clay exhibits a more complicated response. Clay is the most dispersive of rock components, because of the platy nature of the constituent minerals which gives the water trapped between clay particles a large surface-to-volume ratio and, consequently, a large capacitance and a high permittivity. The ability to absorb ions on the exposed surfaces plays a role as well. By testing pure clay samples, we have seen that the SMD model works properly if the CEC is low. Medium/high CEC clays can be modeled too, but only if the salinity of the saturant water is large enough. The critical salinity value lies somewhere between 10 and 30 ppk (**Fig.7**). Certainly, there is a strong connection between this experimental critical salinity and the salinity above which the thickness of bound water becomes the lowest possible (that happens when the diffuse layer vanishes: according to theory, at around 20 ppk at room temperature [**7**]).

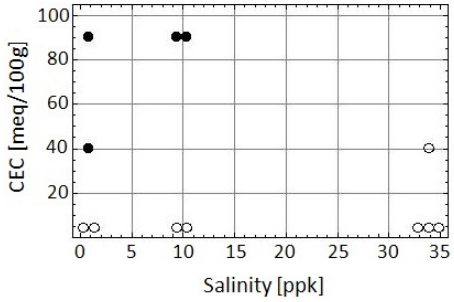

Figure 7: SMD validity study for pure clay samples. Filled circles represent scenarios where SMD fails while open circles where SMD is reliable. It can be seen that the SMD model properly works in the low CEC range (despite the salinity values) and for medium/high CEC only when the brine salinity is large.

All SMD-modellable rocks have in common the fact that dielectric dispersion is basically governed by texture: interfacial polarization is the dominant mechanism in these systems. This type of polarization exhibits resonance frequencies that are directly proportional to water conductivity (σ_w) and, therefore, when permittivity and conductivity spectra measured at different brine salinities are re-plotted as a function of $\omega\varepsilon_0/\sigma_w$ (instead of $f = \omega/2\pi$) the curves collapse all onto one single curve (**Fig.8a**) (see also [**8**]). Actually, the SMD model shows the same type of invariance. Medium/high CEC clays saturated with low salinity brine, on the contrary, do not behave this way (**Fig.8b**).

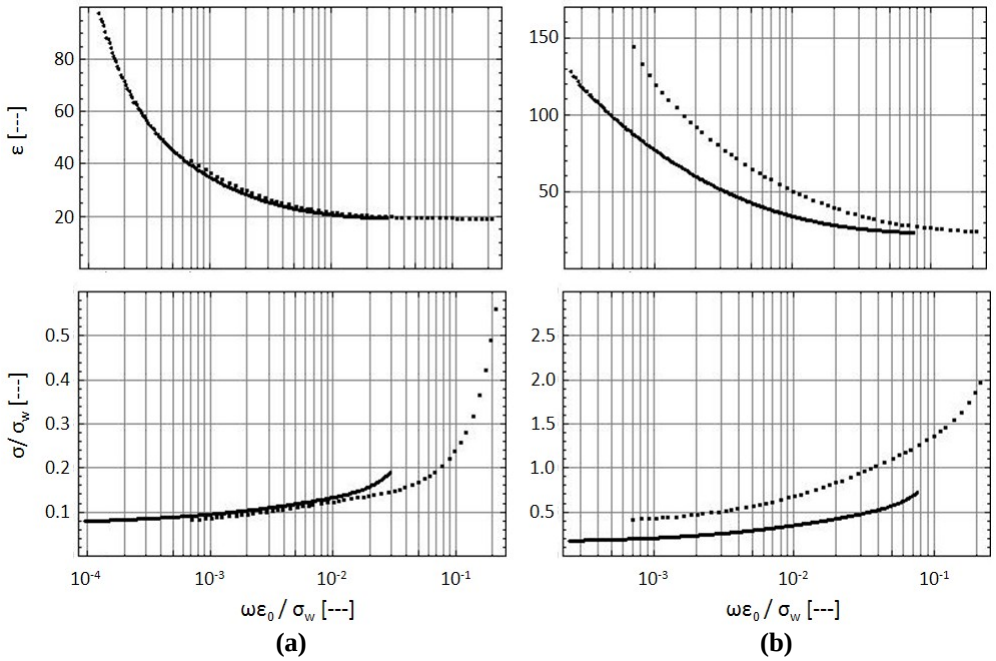

Figure 8: Examples of dielectric scaling. (**Fig.8a**): permittivity and conductivity spectra measured on two low CEC kaolinite samples saturated with different NaCl brines (dotted curves: 1 ppk; solid curves: 30 ppk). (**Fig.8b**): dielectric spectra of two high CEC montmorillonite samples (dotted curves: 1 ppk; solid curves: 10 ppk).

In the latter systems (**Fig.8b**), dispersion is governed by mechanisms that are more intimately related to the characteristics of bound water: the double layer is thicker and the application of an oscillating electric field causes the counterions to move around the clay particles either interacting with the bulk water (diffuse layer polarization) or remaining

confined within the Stern layer (bound layer polarization); another mechanism playing a role because of the non-negligible bound water thickness is membrane polarization [**4, 6**]. In all these processes, resonance effects are generated within the bound water itself, the dielectric response is no longer $\omega\varepsilon_0/\sigma_w$-invariant and, as a result, the SMD model fails.
The reservoir samples analyzed in this study contain clays, in particular smectite, which is a high CEC clay. The best fits to the data are generally good, as shown in the example in **Fig.9**, and the inverted values of water filled porosity and salinity are consistent with the true ones (**Fig.10a** and **10b**). Also the μ parameter (**Fig.10c**) looks reasonable: notice that the shales (clay content from 35 to 50%) exhibit larger μ values than the shaly-sands (clay content less than 20%). The applicability of the SMD model in spite of the high CEC values of these samples is due to the fact that salinity is above 30 ppk, i.e. it is higher than the aforementioned critical value. Intrinsic bound water polarization effects are consequently negligible in these rocks.

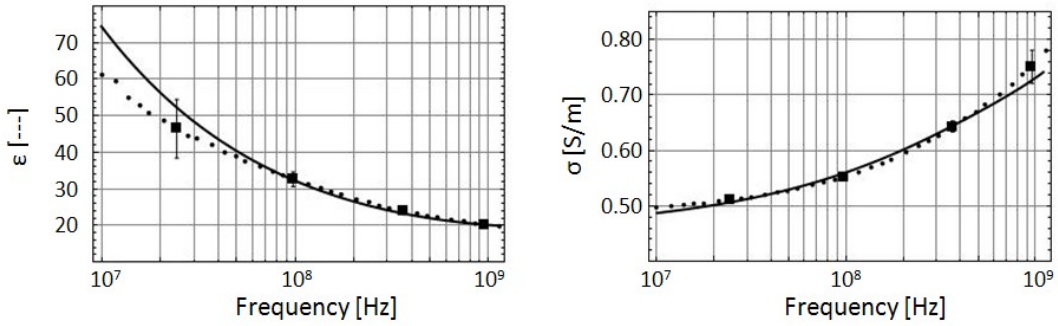

Figure 9: SMD model fit on one reservoir sample: permittivity (left) and conductivity (right).

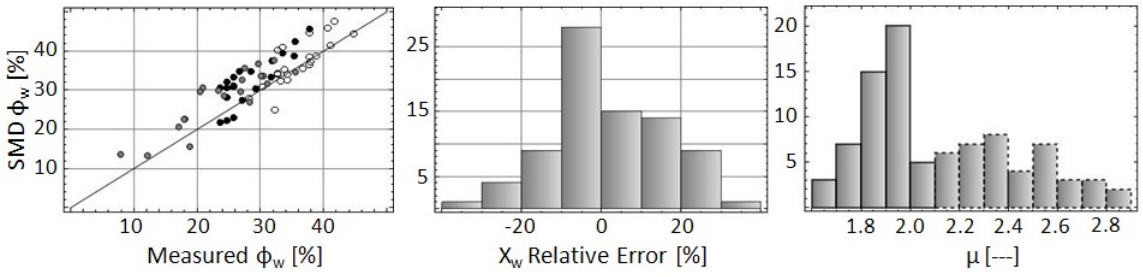

(a) **(b)** **(c)**

Figure 10: SMD inversion results for water-filled porosity, salinity and μ parameter on reservoir samples. In **(Fig.10a)**, filled circles are shales (with a mean absolute error, MAE, of 4%), open circles are fully water saturated shaly-sands (MAE = 2%) while gray circles represent partially saturated shaly-sands (MAE = 5%). **(Fig.10b)** collects the relative errors in salinities with respect to the nominal ones (30 and 36 ppk): a 20% relative error is considered as acceptable. The histogram in **(Fig.10c)** separates the inversion results for μ between shaly-sands (continuous edges) and shales (dashed edges).

FROM DISPERSION TO PETROPHYSICS

A sensitivity analysis of the parameters involved in the SMD model reveals that μ is the parameter that mostly drives the dielectric dispersion, both in permittivity and conductivity. Because dielectric dispersion is prevalently associated with clay, the more clay we have, the more dispersion we should observe, the higher the μ parameter. We

have seen that above a critical salinity, dielectric dispersion is essentially a texture-related phenomenon and high pore surface-to-volume ratios generate larger dispersions (see also [**9**]). Because there is a strong correlation between specific surface area and CEC (**Fig.11a**), a good correlation should be expected also between CEC and μ. This is, in fact, what we observe (**Fig.11b**) and the conclusion is that the SMD model gives indirect access also to Cation Exchange Capacity through a suitable function that fits the data.

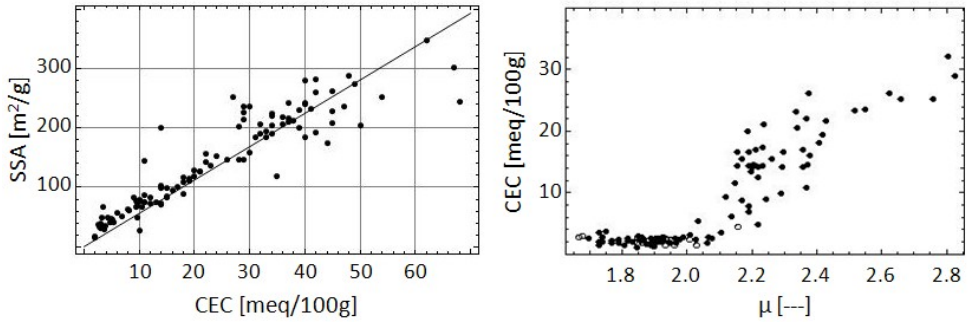

(a) **(b)**

Figure 11: Correlation between specific surface area and CEC as given in [**10**], $R^2 = 0.81$, **(Fig.11a)** and experimental correlation between CEC and μ parameter including partially saturated samples (open circles in the low CEC range) obtained from our study **(Fig.11b)**. It should be noted that the model starts to be really CEC-predictive for $\mu > 1.95$.

Cation Exchange Capacity is one of the petrophysical parameters that better discriminates clay, however for petrophysical interpretation it is important to determine the volume occupied by clay bound water and/or the volume fraction of clay in the probed rock. The path described in [**7**] could represent a safe way to address the issue. The starting point is to know the clay surface area in contact with the water fraction that is actually related to clay charge. The experimental data of **Fig.11a** can be used to obtain specific surface area (SSA) from CEC, namely $SSA \approx \alpha CEC$ with α the constant of proportionality. Normalizing to porosity, rather than density, yields the clay surface per unit pore volume (SSA_{PV}). Now, let x_d be thickness of a clay water layer. At their closest approach, the counterions are located with their centers lying on what is called the Outer Helmholtz Plane (OHP) at a fixed distance x_H from the clay surface. The distance of the OHP is $x_H \approx 6.2\ \AA$ at room temperature. The layer thickness x_d mainly depends on salinity and the salt concentration at which this thickness matches the OHP distance is about 20 ppk. When salinity is above 20 ppk, clay water thickness matches x_H and the volume of clay bound water, per unit bulk volume, should be reasonably approximated by $V_{cw} \approx SSA_{PV}\, x_H\, \phi_T$. The latter is exactly the situation in which SMD for shaly-sands works. Further physically-based assumptions together with a good knowledge of rock mineralogy also yield a possible estimation of the clay volume.

APPLICATION TO REAL CASES

In order to fully illustrate the information provided by the novel dielectric interpretation approach, two cored intervals, (**A**) and (**B**), with different characteristics and coming from different reservoirs have been chosen.

In both wells the new dielectric dispersion tool [**1**] was run. The tool is pad-mounted with two transmitters and eight symmetrically located receivers working in a longitudinal and transversal mode. It acquires radial information up to 4 inches into the formation. The tool measures rock's dielectric properties at four frequencies between 20 MHz and 1 GHz, providing a measurement of the dielectric dispersion at a 1 inch vertical resolution. After a suitable radial inversion, the final outputs are conductivities and permittivities at each depth and at each frequency. The SMD model transforms these results into petrophysical parameters.
Interval (**A**) comes from an onshore field located in Northern Italy. The well is vertical and was drilled in a gas bearing shaly-sand turbiditic sequence. Formation water salinity is high (around 70 ppk). In **Fig.12** we collect the SMD results.

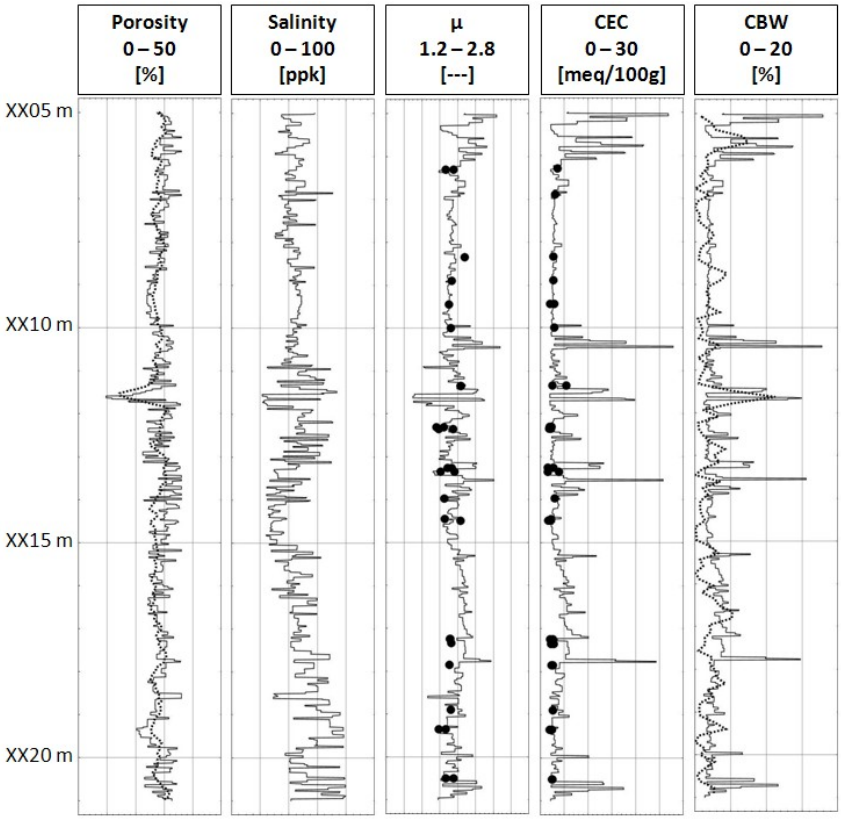

Figure 12: Dielectric-based petrophysical interpretation in case (**A**). Track 1: water-filled porosity from SMD (continuous curve) and total porosity from density-neutron logs (dashed curve). Track 2: fluid salinity from SMD. Track 3: μ parameter comparison (dots comes from experimental measurements on core samples). Track 4: CEC obtained via μ-correlation (dots from experiments). Track 5: clay bound water volume from dielectric dispersion (continuous curve) and from NMR log (dashed curve).

The presented section consists of a thick sand body with sparse shale beds. The first three tracks represent the direct SMD inverted parameters. Water-filled porosity (track 1) is compared with total porosity showing a good correlation in this mostly water-bearing section as expected. In track 2 we can follow the variation of fluid salinity which takes advantage of the shallow depth of investigation of the tool, showing the mixing of

formation water and fresher mud filtrate. A high salinity value implies that invasion is negligible and, therefore, permeability rather low. Under this light, salinity can be also used as a reservoir quality indicator. The μ parameter (in very good agreement with the experiments) in track 3 may be used as a qualitative lithological indicator, see the discussion related to **Fig.10c**. However, for a quantitative estimation, CEC (track 4) and clay bound water volume (track 5) are computed following the correlations in **Fig.11**. The reliability of the results comes from the comparison with laboratory measurements for CEC and with the bound water fraction curve from NMR. It is worth mentioning the high vertical resolution of the dielectric interpretation thanks to the 1 inch resolution of the tool. This will be crucial in very thin layered reservoir as we are going to show.
In example (**B**), the reservoir is extremely complex since the shaly-sand turbiditic sequence is characterized by bed thicknesses that can be even lower than 1 cm. The SMD model still works properly (**Fig.13**).

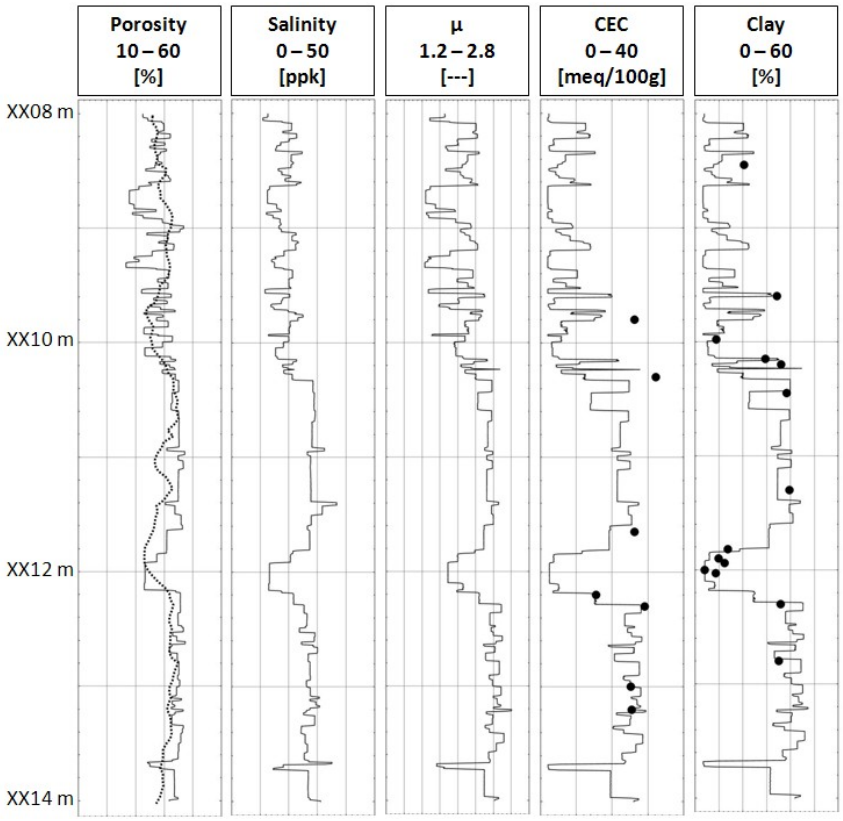

Figure 13: Dielectric-based petrophysical interpretation in case (**B**). Track 1: water-filled porosity from SMD (continuous curve) and total porosity from density-neutron logs (dashed curve). Track 2: fluid salinity from SMD. Track 3: μ parameter from SMD. Track 4: CEC obtained via μ-correlation (dots from experiments on core samples). Track 5: dry clay volume fraction from dielectric dispersion (continuous curve) and from granulometry measurements (dots represent grain size lower than 2 micron, a commonly accepted definition of clay).

The interval consists of two distinct zones: a thinly laminated section (down to cm scale) from top to about XX10m and a thick silty-shale section inter-bedded with thin silty laminations and split into two sub-zones by a thick sand layer at XX12 m.

The salinity profile in track 2 (formation water salinity is about 35 ppk) shows a deeper fresh mud invasion in the sand beds (suggesting a higher permeability, as expected). CEC and dry clay fraction (track 4 and 5) obtained from μ (track 3) are again in good agreement with experiments. More details on the dielectric-based interpretation of this interval can be found in [**11**]. This second example confirms the validity of the proposed approach. Moreover it provides an insight on this innovative methodology for a complete petrophysical characterization of thin layered reservoirs, where conventional analysis has often proved to be meaningless (due to the poor vertical resolution of the majority of standard logging tools).

CONCLUSIONS

Electrical conductivity and dielectric permittivity data measured at four different frequencies in the 20 MHz – 1 GHz range can be inverted to obtain water-filled porosity, water salinity and a clay-related parameter that is intimately related to Cation Exchange Capacity. The physical model behind this calculation was proposed by Stroud, Milton and De for clay-free, fully water saturated rocks [**2**]. We have shown that the model, with very minor changes, works properly also on partially water saturated shaly sands with salinities above 30 ppk. The model has been developed with the aim to maximize the value of a new dielectric dispersion logging tool in thin layered sand-shale reservoirs. The validity and strength of the aforementioned approach have been illustrated by means of two case studies.

REFERENCES

1. M. Hizem, H. Budan, B. Devillé, O. Faivre, L. Mossé, M. Simon, “Dielectric dispersion: a new wireline petrophysical measurement”, SPE paper 116130 (2008).
2. D. Stroud, G. W. Milton, B. R. De, “Analytical model for the dielectric response of brine-saturated rocks”, Phys. Rev. B 34, 5145 (1986).
3. N. Wagner, K. Kupfer, E. Trinks, “A broadband dielectric spectroscopy study of the relaxation behavior of subsoil”, ISEMA, 1-8 (2007).
4. O. A. L. de Lima, M. M. Sharma, “A generalized Maxwell-Wagner theory for membrane polarization in shaly sands”, Geophyiscs, v. 57, no. 3, p. 431-440 (1992).
5. D. Or, J. M. Wraith, "Temperature effects on soil bulk dielectric permittivity measured by time domain reflectometry: a physical model”, Water Resour. Res. 35: 371-383 (1999).
6. T. L. Chelidze, Y. Gueguen, “Electrical spectroscopy of porous rocks: a review – I. Theoretical models”, Geophys. J. Int., v. 137(1), p. 1-15 (1999).
7. C. Clavier, G. Coates, J. Dumanoir, “Theoretical and experimental bases for the dual-water model for interpretation of shaly sands”, SPE J, 24, p. 153-167 (1984).
8. W. E. Kenyon, “Texture effects on megahertz dielectric properties of calcite rock samples”, J. Appl. Phys., 55, 8 (1984).
9. R. J. Knight, A. Nur, “The dielectric constant of sandstones, 60 kHz to 4 MHz”, Geophysics, v. 52, no. 5, p. 644-654 (1987).
10. J. G. Patchett, “An investigation of shale conductivity”, SPWLA, 16th Am. Log. Symp. Trans., paper V (1975).
11. M. Pirrone, N. Bona, M. T. Galli, F. Pampuri, O. Faivre, M. Han, M. Hizem, L. Mossé, “An innovative dielectric dispersion measurement for better evaluation of thin layered reservoirs applied in a south Italy well”, OMC paper FORM/02 (2011).